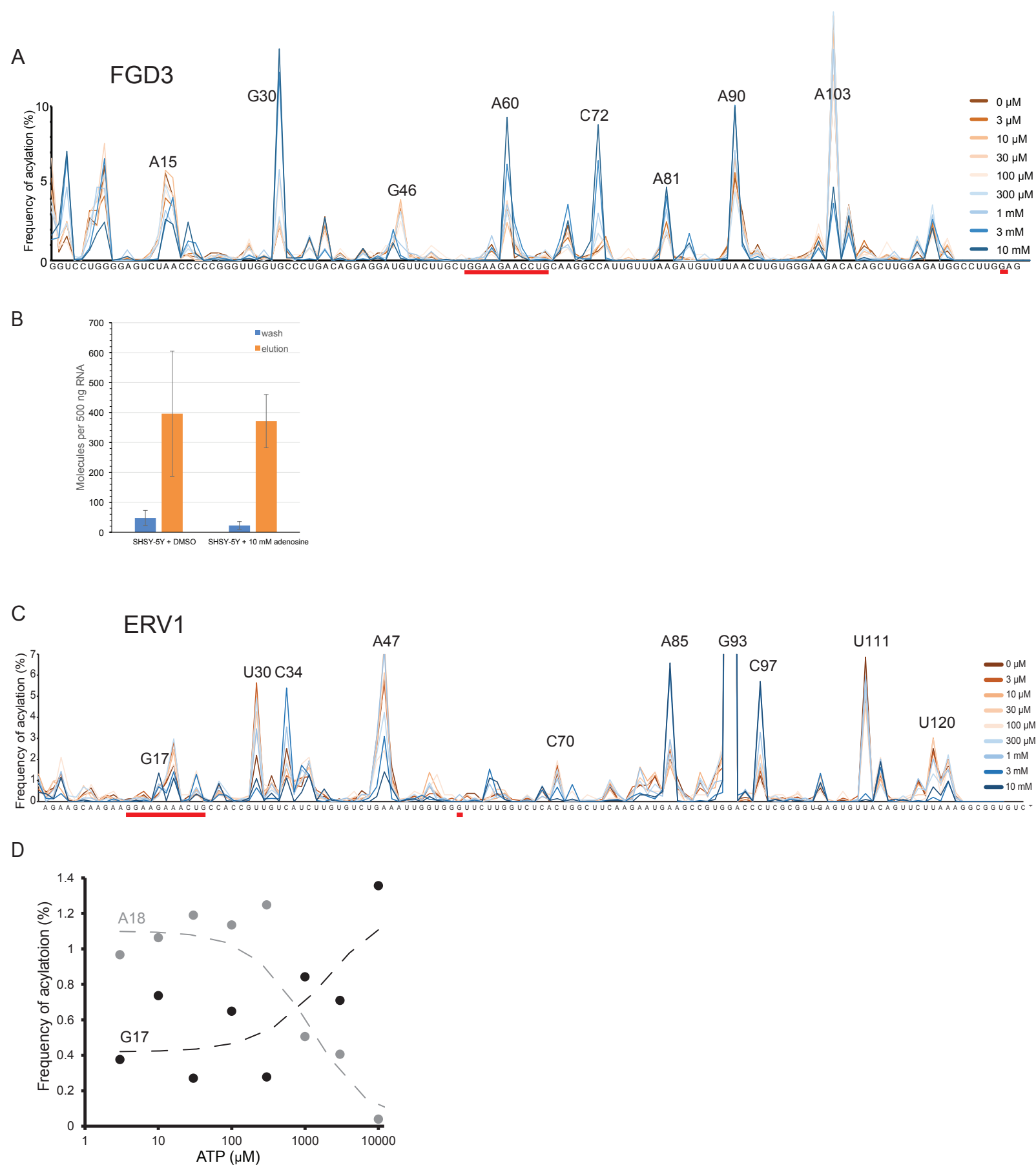


## **Supplementary Information**

### **Multiplex aptamer discovery through Apta-Seq and its application to ATP aptamers derived from human-genomic SELEX.**

Michael M. Abdelsayed<sup>1,§</sup>, Bao T. Ho<sup>2,§</sup>, Michael M. K. Vu<sup>3,§</sup>, Julio Polanco<sup>1</sup>, Robert C.  
Spitale<sup>2,3</sup>, and Andrej Lupták<sup>1,2,3\*</sup>



**Figure S1. Related to Fig.2.** Apta-Seq data of previously reported human FGD3 and ERV1 aptamers (A) Trace of acylation frequency for the FGD3 aptamer with varying ATP concentrations from no ATP to 10 mM ATP. The adenosine binding motif is underlined in red. (B) Binding of ATP beads by the FGD3 sequence measured using RT-qPCR of 500 ng of total RNA isolated from the human SHSY-5Y cell line incubated in absence (DMSO) or presence of 10 mM exogenous adenosine. The aptamer quantities are expressed as the number of molecules in the last wash and ATP elution fractions out of the starting 500 ng of total cellular RNA. Error bars are s.e.m. of three qPCR replicates. (C) Trace of acylation frequency for the ERV1 aptamer with varying ATP concentrations from no ATP to 10 mM ATP. The adenosine binding motif is underlined in red. (D) Binding isotherms of the ERV1 aptamer modeled from the acylation

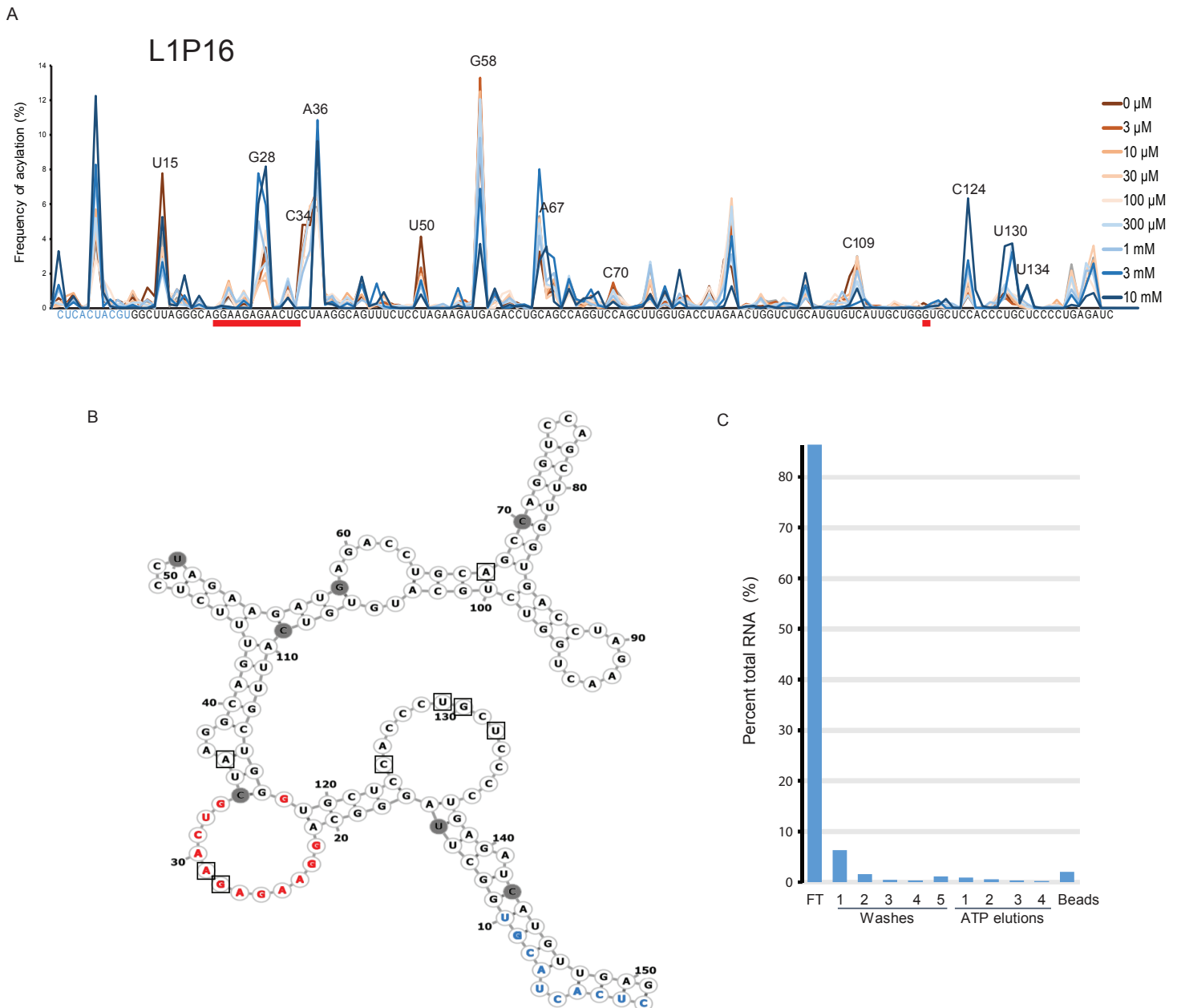


**Figure S2. Related to Fig.4.** Apta-Seq data of the human L1PA16 adenosine aptamer. (a) Trace of acylation frequency for the L1PA16 aptamer with varying ATP concentrations from no ATP to 10 mM ATP. The adenosine binding motif is underlined in red. (b) Secondary structure of the L1PA16 aptamer with ATP binding loop in red and nongenic regions in blue. Nucleotides boxed in black indicate positions that show an increase in acylation with increasing ATP concentration whereas those that show a decrease are filled in grey. (c) Elution profile of the G26A mutant of the L1PA16 aptamer, showing lack of binding to ATP beads (compared to the binding profile of the wild-type sequence shown in Fig. 4E). Wash 5 was incubated longer than wash 4, and equally long as the elutions, resulting in slight increase of RNA in the fraction.

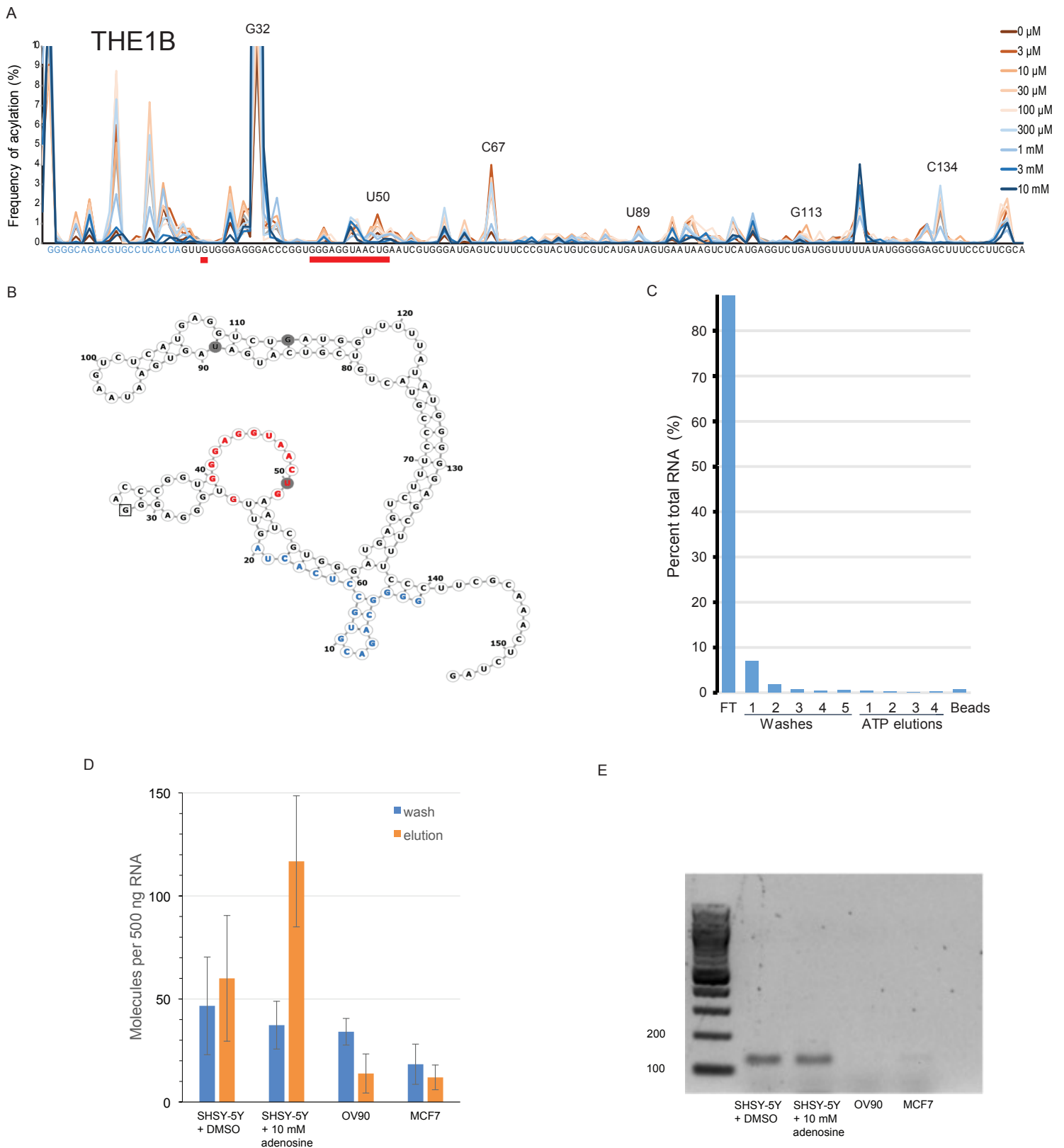


**Figure S3. Related to Fig.4. Human THE1B adenosine aptamer.** (A) Trace of acylation frequency for the THE1B aptamer with varying ATP concentrations from no ATP to 10 mM ATP. The adenosine binding motif is underlined in red. (B) Secondary structure of the THE1B aptamer with ATP binding loop in red and nongenomic regions in blue. Nucleotides boxed in black indicate positions that show an increase in acylation with increasing ATP concentration while those that show a decrease are filled in grey. (C) Elution profile of the G24U mutant showing lack of binding to ATP (compare with Fig. 4F for the binding profile of the wild-type sequence). (D) ATP beads binding by the THE1B sequence measured using RT-qPCR of 500 ng of total RNA isolated from the human cell lines indicated below the graph. The aptamer quantities are expressed as the number of molecules in the last wash and ATP elution fractions out of the starting 500 ng of total cellular RNA. Error bars are s.e.m. of three qPCR replicates. (E) Agarose gel electrophoresis of the THE1B aptamer amplified from the elution fractions in the indicated cell lines.